

(Polypyridyl)ruthenium(II) Complexes Based on a *Back-to-Back* Bis(pyrazolyipyridine) Bridging Ligand

Frank Schramm,^[a] Rajadurai Chandrasekar,^{[a],[‡]} Thomas A. Zevaco,^[b] Manfred Rudolph,^[c] Helmar Görls,^[c] Wolfgang Poppitz,^[c] and Mario Ruben^{*[a]}

Keywords: Ruthenium / Back-to-back ligands / N ligands / Bridging ligands

Two (polypyridyl)ruthenium(II) complexes, [(tpy)Ru^{II}(L)](PF₆)₂ (**1**) and [(tpy)Ru^{II}(L)Ru^{II}(tpy)](PF₆)₄ (**2**) {tpy is 2,2':6',2''-terpyridine and L is 1,4-bis[(2,6-dipyrazol-1-yl)pyrid-4-yl]benzene}, were synthesised and studied in view of their electrochemical and photophysical properties. The structural characterisation of **1** and **2** was carried out by ¹H and ¹³C NMR spectroscopy, MALDI-TOF/ESI mass spectrometry and single-crystal X-ray analysis. The spectro- and electrochemical consequences of the introduction of 2,6-dipyrazol-1-ylpyridine coordinating units into Ru^{II} polypyridyl complexes were investigated by UV/Vis, low-temperature emission

spectroscopy and square-wave voltammetry. It was shown that ligand L can be used as a *back-to-back* bridging ligand in the construction of multinuclear ruthenium(II) ion arrays. In comparison to the widely used 2,2':6',2''-terpyridyl system, the 2,6-dipyrazol-1-ylpyrid-4-yl unit was found to act as a relatively strong σ -donor and weak π -acceptor ligand which allows its use as a structural and electronic alternative in multinuclear architectures.

(© Wiley-VCH Verlag GmbH & Co. KGaA, 69451 Weinheim, Germany, 2009)

Introduction

During the last decades, ruthenium(II)-based polypyridyl complexes have been the object of an active field of research.^[1,2] Light-absorbing and light-emitting properties of ruthenium complexes elevate them to the ranks of prominent candidates for applications dealing with light-driven conversion processes such as, e.g., artificial photosynthesis,^[3] photocatalytic production of hydrogen,^[4] vectorially controlled energy transfer,^[5] photoactivated reactions,^[6] dye-sensitised solar cells,^[7] photomolecular switches,^[8] as well as ion-specific sensing systems,^[9] and other related molecular devices.^[10]

Oligonuclear ruthenium complexes are frequently used to enhance photochemical and photophysical properties of photoactive systems by antenna-like light-harvesting.^[11–13]

The design of multinuclear metal complexes requires organic molecules which can act as bridging ligands, e.g. aro-

matic bis(terdentate) or bis(bidentate) *back-to-back* coupled polypyridines. In particular, ligand systems involving the bis(2,2':6',2''-terpyridin-4'-yl) {tpy} moiety have been used extensively in the construction of multimetallic molecular coordination arrays and artificial antenna systems.^[14–28]

As there are only few examples of known bis(terdentate ligand) complexes that are not based on tpy systems,^[29–33] we decided to investigate the suitability of the equally terdentate 2,6-dipyrazol-1-ylpyridine coordination unit as a bridging ligand motif.^[34] Towards this goal, the multicoordination behaviour of the *back-to-back* ligand 1,4-bis[(2,6-dipyrazol-1-yl)pyrid-4-yl]benzene (L) was studied exemplarily in the synthesis of mono- and binuclear Ru^{II} polypyridyl complexes involving L. Thereby, it was necessary to apply a *mixed-ligand approach* incorporating both bridging ligand L and peripheral tpy ligands.

Herein, we report on the synthesis, X-ray structure, NMR spectroscopic characterisation, optical and electrochemical properties of the mononuclear complex [(tpy)Ru(L)](PF₆)₂ (**1**) and its binuclear equivalent [(tpy)Ru(L)Ru(tpy)](PF₆)₄ (**2**), elucidating the electronic properties of ligand L.

Results and Discussion

Synthesis of Complexes [(tpy)Ru(L)](PF₆)₂ (**1**) and [(tpy)Ru(L)Ru(tpy)](PF₆)₄ (**2**)

The synthesis of complexes **1** and **2** was carried out as described in Scheme 1, whereby the bridging ligand L was

[a] Institut für Nanotechnologie, Forschungszentrum Karlsruhe GmbH,
P. O. Box 3640, 76021 Karlsruhe, Germany
E-mail: mario.ruben@int.fzk.de

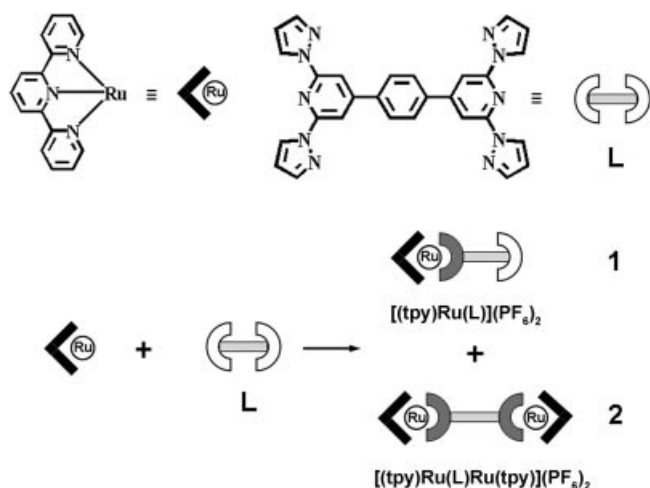
[b] Institut für Technische Chemie – Chemisch-Physikalische Verfahren, Forschungszentrum Karlsruhe GmbH,
Karlsruhe, Germany

[c] Friedrich-Schiller-Universität Jena, Institut für anorganische und analytische Chemie
August-Bebel-Str. 2, 07743 Jena, Germany

[‡] Present address: School of Chemistry, University of Hyderabad, Central University
P. O. Box, Gachi Bowli, Hyderabad 500046, India

Supporting information for this article is available on the WWW under <http://www.eurjic.org> or from the author.

used as described recently.^[35] One equivalent of ligand L was treated with 1.5 equiv. of an in situ prepared tetrafluoroborate salt of mono(2:2',6':2''-terpyridyl)ruthenium.^[5d] After 12 h of reaction time at 120 °C in dmf, the resulting red-orange solid was purified by column chromatography on silica gel, from which the two different nitrate salts of complex **1** and **2** were obtained. Red-brown coloured prismatic single crystals of complex **1**·(NO₃)₂ were suitable for X-ray diffraction studies.



Scheme 1. Schematic presentation of the synthesis of [(tpy)Ru(L)](PF₆)₂ (**1**) and [(tpy)Ru(L)Ru(tpy)](PF₆)₄ (**2**).

Anion exchange was carried out by dissolving complexes **1** or **2** in methanol/water (4:1), respectively. Adding aqueous NH₄PF₆ solution initiated immediate precipitation of the respective PF₆ salt complex material. If not otherwise noted, the PF₆ salt complexes were used in the investigations without further purification.

NMR Spectroscopic Data

Figure 1 shows the ¹H NMR spectra of ligand L and of complexes **1** and **2** in [D₆]dmsO solution. In all cases, ¹H and ¹³C NMR spectra give well-resolved signals. As ligand L is poorly soluble in deuteriated dimethyl sulfoxide, [D₆]dmsO, the spectrum was taken at 70 °C. Since L is a covalent, aprotic ligand, it is supposed that temperature dependence has only a minor influence on the chemical shifts.^[37]

Ligand L itself displays a clear D_{2h} symmetry in solution, giving five signals for the ¹H atoms (Figure 1a) and eight signals for the ¹³C atoms. The presence of *s-trans*, *trans* conformations of the pyrazolyl groups with respect to the central pyridine groups can be concluded from the observed chemical shifts for L in the uncoordinated form (Figure 1a).^[38,39] Due to the substitution at the N¹ atom of the pyrazole, the chemical shift of H_{pz5} is largely downfield-shifted. This shift is attributed to the interaction of the H_{pz5} proton with the electron density of the pyridine lone pair, causing local deshielding of the magnetic field.

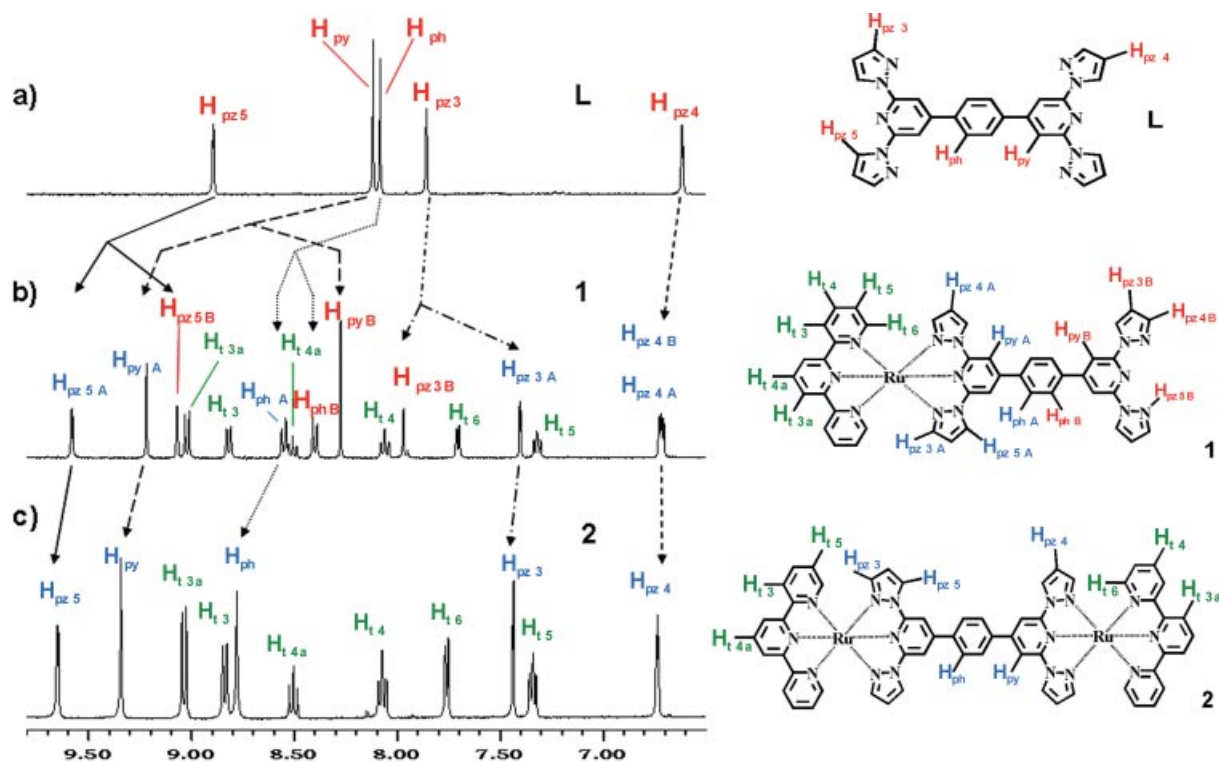


Figure 1. Representation of the aromatic region of the ¹H NMR spectra (a) of L in [D₆]dmsO together with the indication of the observed shifts of the aromatic protons upon complexation by (b) one or (c) two Ru(tpy) units, yielding complex **1** or **2**, respectively (left). The assignment codes of the protons are depicted in the structural formulae (right).

Extensive NMR spectroscopic studies such as two-dimensional techniques – ^1H , ^1H -correlation spectroscopy (H,H-gCOSY), and ^1H , ^{13}C short-range (gHSQC) and long-range correlation spectroscopic (gHMBC) techniques – were employed to achieve full assignment of all signals (see also Supporting Information).

The ^1H NMR spectrum of mononuclear complex **1** shows that the symmetry of ligand **L** in **1** is reduced to C_{2v} symmetry, which results in two sets of NMR signals belonging to two subunits of **L**. Accordingly, ten signals are observed in the ^1H NMR spectrum for **L**, in addition to the terpyridine-related signals (Figure 1b, *green* colour code). Since upon complexation of **L**, rotation of the pyrazole residues into the *s-cis,cis* conformation has to occur, a strong difference in the chemical shifts of the pyrazolyl protons is observed, discriminating the different coordination states of **L**. The ^1H NMR signals of **1** split into a “chelated” (*blue* colour code in Figure 1b) and an “unchelated” (*red* colour code in Figure 1b) set of signals. In particular, the signals H_{pyA} and H_{pz5A} show downfield shifts of 0.94 ppm and 0.51 ppm with respect to their unchelated “B” equivalents. This can be explained by the forced structural vicinity of these two protons, which causes deshielding of both. On the other hand, H_{pz3A} receives an upfield shift of 0.47 ppm in comparison to H_{pz3B} , which is ascribed to a redistribution of electron density at this position due to metal complexation. As expected, the ^{13}C NMR spectrum of **1** exhibits the 16 signals of the asymmetrically coordinated ligand **L**.

Upon introduction of the second (terpyridyl)ruthenium(II) moiety, binuclear complex **2** exhibits D_{2h} symmetry. This leads to simplified NMR spectra exhibiting five signals in the ^1H NMR spectrum, featuring the all-chelated situation, and eight signals in the ^{13}C NMR spectrum (Figure 1c).

MALDI-TOF and ESI Mass Spectrometric Analyses

Matrix-assisted laser desorption/ionisation-time of flight (MALDI-TOF) mass spectrometric analytical data further confirmed the structural identity of compounds **1** and **2**. The analysis of **1** exhibits a molecular peak at $m/z = 829.7$ $[(\text{tpy})\text{Ru}(\text{L}) - 2\text{H}]^+$ with 100% intensity, which is often accompanied by a peak at $m/z = 802$ with 30% intensity, corresponding to the loss of a “ CH_3N ” or “ HN_2 ” fragment. Similarly, ions like $[(\text{tpy})\text{RuOH}]^+$ at $m/z = 351$ are frequently found in the spectra.

The spectrum of binuclear complex **2** (as the nitrate salt) shows the highest mass peak at $m/z = 1161.7$ with 12% intensity, which corresponds to the singly charged mass of the binuclear complex $[(\text{tpy})\text{Ru}(\text{L})\text{Ru}(\text{tpy}) - 5\text{H}]^+$ lacking five hydrogen atoms and all anions. In fact, the isotope pattern of this peak matches the theoretical values of the natural isotope contribution. The dominating peak in the spectrum at $m/z = 829.2$ with 65% intensity can be attributed to $[(\text{tpy})\text{Ru}(\text{L}) - 2\text{H}]^+$.

Additionally, electrospray ionisation time-of-flight (ESI-TOF) measurements were applied to the PF_6 salts of both

1 and **2**. Complex **1** shows different peaks of the molecular ion as $[\mathbf{1}\cdot\text{PF}_6]^+$ at $m/z = 976.13$, $[\mathbf{1}\cdot(\text{PF}_6)_2\cdot\text{PF}_5]^{2+}$ at $m/z = 623.64$ and $[\mathbf{1}]^{2+}$ at $m/z = 415.59$. Similar results were found for complex **2** with ion peaks of $[\mathbf{2}\cdot(\text{PF}_6)_2]^{2+}$ at $m/z = 728.05$, $[\mathbf{2}\cdot\text{PF}_6]^{3+}$ at $m/z = 437.04$ and $[\mathbf{2}]^{4+}$ at $m/z = 291.54$. In general, ESI-TOF leaves the molecular ions of the complexes relatively intact (see also Supporting Information).

Single-Crystal X-ray Structure of **1**

The result of the single-crystal X-ray diffraction studies on complex **1** (as its nitrate salt), at 180 K is depicted in Figure 2. The compound crystallises in the monoclinic space group $P2_1/n$. Four molecules of **1** are included in the unit cell together with four molecules of methanol and eight nitrate counteranions. The bond lengths of the coordination sphere are within the expected range for hexacoordinate ruthenium(II) complexes and vary from 1.974(4) Å (Ru–N12) to 1.992(4) Å (Ru–N3) at the central pyridine rings and from 2.049(4) Å (Ru–N1 and Ru–N11) to 2.087(4) Å (Ru–N5) for the angular nitrogen atoms of the coordinated li-

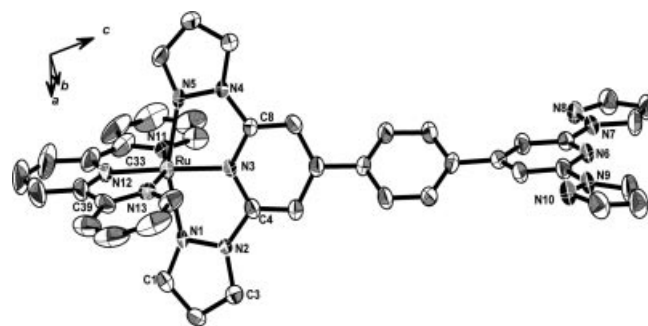


Figure 2. ORTEP plot of the $[(\text{tpy})\text{Ru}(\text{L})]^{2+}$ cation of complex **1** (thermal ellipsoids at the 50% probability level) – nitrate anions, hydrogen atoms and solvent molecules are omitted for clarity.

Table 1. Selected bond lengths and angles of the complex cation **1**.^[a]

Selected distances / Å		Selected angles / °	
Ru–N1	2.049(4)	N1–Ru–N3	78.52(15)
Ru–N3	1.992(4)	N3–Ru–N5	77.77(15)
Ru–N5	2.087(4)	N1–Ru–N5	156.27(14)
Ru–N11	2.054(4)	N11–Ru–N12	79.42(18)
Ru–N12	1.974(4)	N12–Ru–N13	79.64(18)
Ru–N13	2.073(4)	N11–Ru–N13	159.04(17)
N1–N2	1.393(5)	N1–Ru–N11	95.78(16)
N1–C1	1.324(6)	N1–Ru–N12	98.77(16)
N2–C4	1.399(6)	N1–Ru–N13	86.73(15)
N2–C3	1.364(6)	N5–Ru–N11	88.69(16)
N3–C4	1.352(6)	N5–Ru–N12	104.96(16)
N3–C8	1.337(6)	N5–Ru–N13	97.36(16)
N4–C8	1.401(6)	N3–Ru–N12	176.61(17)
N4–N5	1.395(5)	N1–N2–C4	119.0(4)
N4–C9	1.363(6)	N2–C4–N3	110.8(4)
N5–C11	1.326(6)	C4–N3–C8	119.0(4)
N11–C33	1.371(7)	N11–C33–C34	114.0(5)
N12–C38	1.339(7)	C34–N12–C38	123.2(5)
N12–C34	1.358(7)	N12–C38–C39	113.0(4)

[a] Dihedral angles: Ru–py–ph 48.66(9)°, ph–py(free) 29.65(9)°.

gands L and tpy. However, the relatively small bite angle of L [N1–Ru–N5 156.27(14)°] produces a significant constraint of the coordination sphere at the Ru^{II} centre (Table 1).

Within the ligand structure of L, the connecting benzene ring exhibits a dihedral angle towards the chelated pyridine ring of 48.66(9)° and towards the unchelated pyridine ring of 29.65(9)°.

In the case of the binuclear complex **2**, single-crystal X-ray diffraction studies could not be carried out because of the low diffraction quality of the obtained crystals.

Absorption and Emission Spectroscopy

Ruthenium(II) ions comprising chelate ligands with strong π -acceptor properties exhibit interesting photophysical properties.^[1,2,11] Table 2 and Figure 3 display the results of the photophysical measurements for complexes **1** and **2**. Both mononuclear complex **1** and binuclear complex **2** exhibit only minor differences in their absorption behaviour.

Table 2. UV/Vis data for compounds **1** and **2** as the nitrate salts in methanol solution in 1 cm cuvettes.

Complex	IL	¹ MLCT (L) λ /nm (ϵ /M ⁻¹ cm ⁻¹)	¹ MLCT (tpy) λ /nm (ϵ /M ⁻¹ cm ⁻¹)	Emission λ /nm at 100 K
1	308 (84300)	366 (8830)	443 (24900)	605
2	309 (96400)	371 (12750)	453 (44880)	619

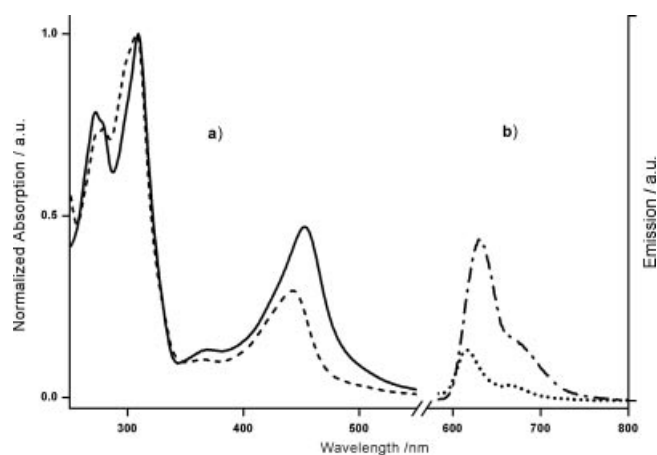


Figure 3. Absorption (room temperature) and emission (100 K) spectra of the PF₆ salts of complexes **1** and **2**. (a) Absorption spectra of complex **1** (dashed line) and complex **2** (solid line) in 10⁻⁵ M methanol/acetonitrile solution. (b) Uncorrected emission spectra at 100 K of complex **1** (dotted line) and complex **2** (dash-dotted line) in a saturated solid matrix consisting of acetonitrile/dmf, 10:1 v/v.

In both complexes, the ligand π - π^* absorptions appear as the most intense peaks of the spectra below 340 nm. Differences between **1** and **2** are observed in the “metal-based”

absorptions. There are two different “metal-to-ligand charge transfer” (MLCT) bands involving each one of the ligand types tpy and L. The intensities and maxima of these transitions can be distinguished by comparing the electronic spectra of complexes **1** and **2**.

The tpy-based ¹MLCT band of mononuclear complex **1** (λ = 443 nm) is 45% lower in intensity and displays a hypsochromic shift of 10 nm in comparison with the respective band of binuclear complex **2** (λ = 453 nm). Furthermore, the ¹MLCT band of the chelated 2,6-dipyrazol-1-ylpyridine (bpp) unit of L is located at λ = 366 nm for complex **1** and at λ = 371 nm for complex **2**. The electronic spectra are in agreement with reported values of the homoleptic complexes [Ru(tpy)₂]²⁺ (λ = 476 nm) and [Ru(bpp)₂]²⁺ (λ = 377 nm).^[14,40] In addition, a reported heteroleptic complex of [Ru(ttpy)(dmpp)]²⁺ {where dmpp is 2,6-bis(3,5-dimethyl-*N*-pyrazolyl)pyridine and ttpy is 4'-tolyl-2,2':6',2''-terpyridine} exhibits two different transitions at λ = 359 nm and λ = 457 nm in a very similar way.^[15,22]

In general, the lowest energetic transitions of a Ru^{II}-N₆ coordination compound are directly referred to the promotion of an electron from the highest occupied (metal based) molecular orbital to the lowest unoccupied electronic level of the respective ligand (MLCT).^[1,36,44] In mixed-ligand compounds such as complexes **1** and **2**, different ligands involve different absorption energies from the same initial metal-based orbital. The absorption spectra of complexes **1** and **2** exhibit a higher energetic MLCT band towards L (around 370 nm) and a lower MLCT band towards tpy (around 450 nm) in accordance with literature values.^[14] Thus, it can be deduced that the coordinating bpp moiety in ligand L possesses a higher electron density, causing stronger repulsion for additional electron density in comparison with the structurally similar tpy moiety. This renders L a stronger σ -donor and a weaker π -acceptor than tpy and lowers the overall ligand-field strength of the 2,6-dipyrazol-1-ylpyridine coordination unit in L with respect to the analogous terpyridyl system.

The light-emitting behaviour of complexes **1** and **2** was investigated at reduced temperatures in a solid matrix of acetonitrile/dmf (10:1 v/v). Only at very low temperatures – below 100 K – luminescence could be detected at 605 nm for complex **1** and at 619 nm for complex **2**. In both cases, the intensity of the luminescence increased further upon cooling (see Supporting Information). At low temperature, both complexes exhibit a red-sided shoulder, as it is common for the Franck-Condon progression of most polypyridylruthenium(II) complexes.^[28] As the parent complex [Ru(tpy)₂]²⁺ emits light at an identical wavelength, the luminescence could be assigned to the radiative depopulation of terpyridine-based ³MLCT states in **1** and **2**.^[44]

The weakness at higher temperatures as well as the strong temperature-dependence of the emission may be related to the weak ligand field of the 2,6-dipyrazol-1-ylpyridine coordination unit, which renders the occupation of a stable ³MLCT state less probable and so favours a nonradiative decay through metal-centred states (³MC).^[41]

Table 3. Comparison of the cyclic voltammetric data of the complexes **1** and **2** measured in dmf with (Bu₄N)ClO₄ vs. the ferrocene/ferrocenium couple. All literature values are calculated with a respective reference electrode adaptation according to reference [22].

Complex	$E_{1/2}(\text{ox}) / \text{V}$	$E_{1/2}(\text{red}) / \text{V}$			
1	+0.765	-1.715	-1.865	-2.050	-2.235
2 ^[a]	+0.765	-1.630	-1.713	-1.849	-1.930
[Ru(bpp) ₂] ²⁺ ^[b]	+0.866	-2.044			
[(dmpp)Ru(tpy)] ²⁺ ^[c]	+0.74	-1.66			
[Ru(tpy) ₂] ²⁺ ^[d]	+0.96	-1.36			
[(ttpy)Ru(tpy-ph-tpy)] ²⁺ ^[e]	+0.87	-1.62	-1.84		
[(ttpy)Ru(tpy-ph-tpy)Ru(tpy)] ⁴⁺ ^[f]	+0.89	-1.56	-1.83		

[a] Peak separations have been determined by fitting simulated square-wave voltammograms (SWVs) to experimental ones excluding the region around the adsorption peak at -1.9 V (see Supporting Information). [b] Values taken from ref.^[14] measured vs. SSCE. [c] Values taken from ref.^[40] measured vs. SCE. [d] Values taken from ref.^[18] [e] Complex [(ttpy)Ru(tpy-ph-tpy)][PF₆]₂ values vs. SCE taken from ref.^[19c,19d] [f] Complex [(ttpy)Ru(tpy-ph-tpy)Ru(tpy)][PF₆]₄ values vs. SCE taken from ref.^[19a,19d]

Electrochemical Data

The results of the electrochemical analysis obtained by cyclic voltammetry and square-wave voltammetry of complexes **1** and **2** are summarised in Table 3. As the complexes are poorly soluble in acetonitrile, dmf solutions with tetra-*n*-butylammonium perchlorate as electrolyte were used.

In both complexes, mononuclear **1** and binuclear **2**, the first oxidation waves occur at the same half-wave potential of $E_{1/2} = +0.765$ V and are fully reversible. Integration of the peak area of the oxidation half-wave curves implies a single-electron oxidation in the case of **1** and a two-electron oxidation in the case of **2**, under the assumption that the diffusion coefficients are equal. To support this assumption, the peak current values of both the reduction (vide infra) and the oxidation of dinuclear complex **2** were compared. As a result, the oxidation wave of complex **2** exhibits a current value that is double that of the single-electron reductions, which clearly supports the above argumentation (see Supporting Information).

In comparison to the homoleptic parent complexes Ru(tpy)₂ [$E_{1/2} = +0.96$ V] and Ru(bpp)₂ [$E_{1/2} = +0.866$ V],^[14,21,40] complexes **1** and **2** are oxidised at less positive potentials. In accordance to the electronic spectra, the introduction of ligand L induces higher electron density onto the ruthenium ion, thus facilitating the oxidation of **1** and **2**. Since complex **2** is twofold oxidised at the same potential like complex **1**, it can be concluded that both ruthenium(II) ions act independently from each other. This electronic situation strongly reminds of the complex [(ttpy)Ru(tpy-ph-tpy)Ru(tpy)][PF₆]₄ [where tpy is 4'-*p*-tolyl-2,2':6,2''-terpyridine and tpy-ph-tpy is 1,4-bis(2,2':6,2''-terpyridin-4'-yl)benzene] involving the analogous tpy bridging ligand.^[19,24]

The reduction of complex **1** reveals four well-separated and equally intense waves, which are fully reversible up to the second reduction. After the third reduction, the electrochemical reversibility is partially lost. The first reduction is found to be at a remarkably high voltage of $E_{1/2} = -1.715$ V, which is close the average value for the parent complexes [Ru(bpp)₂]²⁺ and [Ru(tpy)₂]²⁺. However, it is still more cathodically shifted as the value reported for the mixed-ligand complex [Ru(bpp)(tpy)]²⁺ (see Table 3 and Supporting Information).^[40] In accordance with the results of absorption

spectroscopy, the first reduction of complex **1** can be directly correlated with the electronic transition with lowest energy – the ¹MLCT transition onto the tpy ligand. Further reductions follow at -1.865, -2.050 and -2.235 V. These values cannot unambiguously be assigned to a specific ligand reduction, as the repulsion of an already negatively charged tpy ligand competes against the electron density of the bpp moiety. Since the absorption spectroscopy of **1** shows that the ¹MLCT onto ligand L is around 0.5 eV higher in energy than the respective ¹MLCT onto the tpy ligand, the first reduction of ligand L is found at more cathodic potentials than $E_{1/2} = -1.865$ V.

The reduction of complex **2** exhibits four fully reversible and equally intense reductions that are not well separated, and the fourth reduction is overlaid with an additional adsorption peak. The fact that all four reductions show equal values of the peak currents in comparison with the peak currents of the reductions of complex **1** allows for the interpretation that all are single-electron processes. The fitting of the reduction waves allows the separation of the respective half-wave potentials: The first reduction wave of complex **2** appears at $E_{1/2} = -1.630$ V, which corresponds to an anodic shift of $\Delta E_{1/2} = 85$ mV in comparison with the first reduction of complex **1**. Again, this first reduction can be attributed to the reduction of one tpy ligand. Further increase in the cathodic potential results in three additional reduction waves in **2** at values of $E_{1/2} = -1.713$, -1.849 and -1.930 V. The second reduction is again proven to be a one-electron process exhibiting a small cathodic shift of $\Delta E_{1/2} = 83$ mV with respect to the first reduction. Thus, this wave can be assigned to the reduction of the second tpy ligand of **2**. Apparently, on the reduction side, a weak communication via the metal ions and the bridging ligand L needs to be considered, which is in clear distinction to the parent tpy-based *back-to-back* ligand (see Supporting Information).^[42] The third and fourth reduction in complex **2** cannot be ascribed with satisfactory certainty, but a reduction of ligand L is suggested.

Conclusions

Two *mixed-ligand* ruthenium(II) complexes, [(tpy)Ru^{II}(L)](PF₆)₂ (**1**) and [(tpy)Ru(L)Ru(tpy)](PF₆)₄ (**2**), involving

the *back-to-back* ligand 1,4-bis[(2,6-dipyrazol-1-yl)pyrid-4-yl]benzene (L) were synthesised. Both complexes were fully characterised by NMR spectroscopy, MALDI-TOF/ESI mass spectrometric analysis and UV/Vis absorption spectroscopy. Furthermore, the molecular structure of the mononuclear complex **1** was determined by single-crystal X-ray diffraction methods, and the spectro- and electrochemical behaviour of both complexes was studied. The appearance of a low-temperature luminescence of the ruthenium-tpy backbone is strongly connected with the strong σ -donor behaviour of ligand L, which causes a weak ligand field and probably inhibits the stabilisation of the tpy-based $^3\text{MLCT}$ at high temperatures. The presence of the coordinating dipyrazol-1-ylpyridyl subunit in ligand L has a marked influence on the chemical properties of the coordination compounds in comparison with the related bis(terpyridyl)benzene systems.^[16,43,44] The substitution of the outer 2-pyridyl residues by 1-pyrazolyl residues results in major changes of the electron-donating capability of the coordinating unit, making the coordinating 2,6-dipyrazolylpyridine units of L act electronically as relatively strong σ -donors and weak π -acceptors.^[45] The electrochemical investigation of the homobimetallic complex **2** indicates the ability of ligand L to mediate weak communication between the peripheral moieties of the complex. It was shown that the *back-to-back* ligand 1,4-bis[(2,6-dipyrazol-1-yl)pyrid-4-yl]benzene (L) can be used as a new bridging ligand system in the construction of multinuclear metal ion coordination arrays, a property which is under current investigation in surface-confined self-assembly studies.^[46]

Experimental Section

Ligand L was synthesised by following a procedure reported previously.^[35] For the synthesis of the complexes, $\text{Ru}(\text{tpy})\text{Cl}_3$ ^[36] was treated with AgBF_4 in acetone prior to use in order to increase its reactivity towards complexation. The Ru precursor was synthesised in dmf with a $\text{Ru}(\text{tpy})/\text{ligand}$ molar ratio of 1.5:1 to support the formation of both mononuclear complex **1** and binuclear complex **2**. After 12 h the reaction was stopped, and after evaporation of the solvents in vacuo the mixture was purified by column chromatography on silica. A mixture of acetonitrile, water and an aqueous solution of potassium nitrate was used as eluent. The first red-orange fraction eluted from the column contains the mononuclear complex **1** in 29% yield. As the binuclear complex **2** shows a more polar behaviour towards silica, the nitrate content was increased in order to displace it. This procedure yielded 9% of complex **2**. After removing the eluent, the mixture was slightly heated in methanol. The small amount of potassium nitrate, which dissolved in methanol, was removed from the complex salt by washing with a small portion of water (3 mL), and the residual red to orange solids were dried. Another way to separate the complexes from the potassium nitrate is to exchange the anion. Thus a methanol solution of the complex is treated with aqueous ammonium hexafluorophosphate solution, and the fast-precipitating solid is filtered off, washed with water and dried. The PF_6 salts show a decreased solubility in organic solvents. The nitrate salts are well soluble in methanol, dimethylformamide, nitromethane, very well soluble in solvent mixtures with water, and slightly soluble in water and acetonitrile (see Supporting Information).

The NMR spectra of the ligands and of the ruthenium complexes were recorded in solutions in $[\text{D}_6]\text{dmso}$ (Chemotrade, Leipzig) with a Varian Inova 400 spectrometer (Oxford magnet; ^1H : 400 MHz, ^{13}C : 100.54 MHz) with 5 mm probe heads ($^1\text{H}/\text{X}$ inverse detection for the 2D experiments and $^1\text{H}/\text{X}$ -BB direct detection for $^{13}\text{C}/\text{DEPT}135$ experiments). TMS was used as internal standard (^{13}C , ^1H) with different deuterated solvents. The observed chemical shifts δ (in ppm) are then given relative to the residual signal of the solvent. The numbering of the atoms are according to the actual IUPAC nomenclature.^[47]

Cyclic square-wave measurements were performed by employing a 3-electrode technique with a "homebuilt" computer-controlled instrument based on the PCI 6110-E data acquisition board (National Instruments). The experiments were conducted in dimethylformamide (containing 0.25 M tetra-*n*-butylammonium perchlorate) under a blanket of solvent-saturated argon. The ohmic resistance which had to be compensated for was determined by measuring the impedance of the system at potentials where the Faraday current was negligibly small. Experimental SWVs used for data fitting were background-corrected by subtracting the current curves of the blank electrolyte containing the same concentration of supporting electrolyte. The reference electrode was an Ag/AgCl electrode in acetonitrile containing 0.25 M tetra-*n*-butylammonium chloride. As recommended by IUPAC,^[48] all data reported in the paper refer to the ferrocenium/ferrocene couple, which was measured at the end of the experiments. The working electrode was either a platinum disk electrode ($d = 1.7$ mm) or a hanging mercury drop ($m = 2.79$ mg) produced by a CGME instrument (Bioanalytical Systems, Inc., West Lafayette, USA). Theoretical SWVs were simulated by using the DigiElch simulation package available from <http://www.DigiElch.de>. The simulation algorithm used in this program has been described in several publications.^[49]

MALDI-TOF MS data were acquired with a Voyager-DE PRO Bio spectrometry work station. Micro-ESI-MS analyses were performed by Dr. W. Poppitz with a Finnigan MAT 95 XL Trap. ESI-TOF mass spectrometry was carried out by Dr. Oliver Hampe and Dr. Verena Tellström at a micrOTOF-Q II at Bruker Daltonik GmbH, Bremen (Germany). Elemental analyses were carried out by Mikroanalytisches Labor Pascher An der Pulvermühle 1, D-53424 Remagen-Bandorf (Germany). UV/Vis analyses were carried out with a Varian Cary 500 Scan UV/Vis/NIR spectrophotometer. Low-temperature luminescence spectra were recorded by Dr. Sergei Lebedkin with a Fluorolog-3 fluorescence spectrometer (Jobin Yvon).

For the crystal structure determination, the intensity data for the compounds were collected with a Nonius KappaCCD diffractometer, by using graphite-monochromated Mo-K_α radiation. Data were corrected for Lorentz and polarisation effects, but not for absorption effects.^[50,51] The structure was solved by direct methods (SHELXS)^[52] and refined by full-matrix least-squares techniques against F_o^2 (SHELXL-97)^[53]. All hydrogen atoms were included at calculated positions with fixed thermal parameters. All non-hydrogen atoms were refined anisotropically.^[53] Diamond v3.1d (Crystal Impact GbR, Bonn, Germany) was used for structure representations.

[(2,2':6',2''-Terpyridyl)ruthenium]{1,4-bis[(2,6-dipyrazol-1-yl)pyrid-4-yl]benzene}bis(hexafluorophosphate) – [(tpy)Ru^{II}(L)](PF₆)₂ (1**):** ^1H NMR (400 MHz, $[\text{D}_6]\text{dmso}$, 25 °C): $\delta = 6.71$ [t_{d}], $^3J_{\text{H,H}} = 2.8$, $^4J_{\text{H,H}} = 0.8$ Hz, 2 H, pz H(4A)], 6.73 [t_{d}], $^3J_{\text{H,H}} = 2.8$, $^4J_{\text{H,H}} = 0.8$ Hz, 2 H, pz H(4B)], 7.32 [dt], $^3J_{\text{H,H}} = 6.6$, $^4J_{\text{H,H}} = 0.8$ Hz, 2 H, tpy H(5), H(5'')], 7.40 [d], $^3J_{\text{H,H}} = 2.0$ Hz, 2 H, pz H(3A)], 7.71 [dd], $^3J_{\text{H,H}} = 5.6$, $^4J_{\text{H,H}} = 0.4$ Hz, 2 H, tpy H(6), H(6'')], 7.97 [d,

$^3J_{\text{H,H}} = 0.8$ Hz, 2 H, pz H(3B)], 8.06 [dt, $^3J_{\text{H,H}} = 8.0$, $^4J_{\text{H,H}} = 1.2$ Hz, 2 H, tpy H(4), H(4'')], 8.28 [s, 2 H, L-py H(3B), H(5B)], 8.40 [d, $^3J_{\text{H,H}} = 8.4$ Hz, 2 H, L-ph H(B)], 8.51 [t, $^3J_{\text{H,H}} = 8.4$ Hz, 1 H, tpy H(4'')], 8.55 [d, $^3J_{\text{H,H}} = 8.8$ Hz, 2 H, L-ph H(A)], 8.82 [d, $^3J_{\text{H,H}} = 8.0$ Hz, 2 H, tpy H(3), H(3'')], 9.02 [d, $^3J_{\text{H,H}} = 8.0$ Hz, 2 H, tpy H(3'), H(5')], 9.07 [d, $^3J_{\text{H,H}} = 2.4$ Hz, 2 H, pz H(5B)], 9.22 [s, 2 H, L-py H(3A), H(5A)], 9.58 [d, $^3J_{\text{H,H}} = 3.2$ Hz, 2 H, pz H(5A)] ppm. ^{13}C NMR (100 MHz, $[\text{D}_6]\text{dmsO}$, 25 °C): $\delta = 106.96$ [L-py C(3A), C(5A)], 107.22 [L-py C(3B), C(5B)], 109.38 [pz C(4B)], 111.24 [tpy C(4A)], 124.04 [tpy C(3'), C(5')], 124.79 [tpy C(3), C(3'')], 128.14 [tpy C(5), C(5'')], 129.03 [L-ph CH(B)], 129.11 [L-ph CH(A)], 129.14 [pz C(5B)], 134.09 [pz-C(5A)], 136.81 [tpy C(4')], 137.98 [L-ph C(1A)], 138.88 [tpy C(4), C(4'')], 139.45 [L-ph C(1B)], 143.56 [pz C(3B)], 146.59 [pz C(3A)], 149.45 [L-py C(2A), C(6A)], 150.69 [L-py C(4A)], 151.14 [L-py C(2B), C(6B)], 153.16 [L-py C(4B)], 153.53 [tpy C(6), C(6'')], 156.89 [tpy C(2'), C(6')], 159.05 [tpy C(2), C(2'')] ppm. "A" refers to chelated side of L, and "B" to the unchelated side. UV/Vis (NO_3^- salt, MeOH): $\lambda_{\text{max}} = 280$ ($\pi \rightarrow \pi^*$ tpy), 308 ($\pi \rightarrow \pi^*$ L), 365 (w, $^1\text{MLCT}$ towards L), 442 (s, $^1\text{MLCT}$ towards tpy) nm. MALDI-TOF MS: $m/z = 829.7$ ($[\text{C}_{43}\text{H}_{29}\text{N}_{13}\text{Ru}]^+$, $[\text{M} - 2\text{PF}_6 - 2\text{H}]$). ESI-TOF MS (acetonitrile/water, 1:1): m/z (%) = 415.59 (100) $[\text{1}]^{2+}$, 437.04 (9) $[\text{1} \cdot \text{F} - \text{H}]^{2+}$, 631.62 (0.5) $[\text{1} \cdot (\text{PF}_6)_3 - \text{H}]^{2+}$, 976.13 (1) $[\text{1} \cdot \text{PF}_6]^+$. $\text{C}_{43}\text{H}_{31}\text{F}_{12}\text{N}_{13}\text{P}_2\text{Ru} \cdot 0.5\text{C}_6\text{H}_{14}$ (1163.89): calcd. C 47.47, H 3.29, N 15.65, Ru 8.68; found C 47.43, H 3.07, N 15.7, Ru 8.73. Because of the insufficient amount of pure complex $\text{1} \cdot (\text{PF}_6)_2$, the sample used for elemental analysis was precipitated with hexane from a NMR-pure $[\text{D}_6]\text{dmsO}$ solution in order to remove dmsO by extraction with water.

Crystal Data for 1: $[\text{C}_{43}\text{H}_{31}\text{N}_{13}\text{ORu}]^{2+} \cdot 2[\text{NO}_3^-] \cdot 0.75\text{CH}_4\text{O}$, $M_r = 978.93$ g mol $^{-1}$, red-brown prism, size $0.06 \times 0.06 \times 0.05$ mm 3 , monoclinic, space group $P2_1/n$, $a = 12.7803(6)$ Å, $b = 14.1300(7)$ Å, $c = 23.5751(8)$ Å, $\beta = 104.030(3)^\circ$, $V = 4130.3(3)$ Å 3 , $T = -90$ °C, $Z = 4$, $\rho_{\text{calcd.}} = 1.574$ g cm $^{-3}$, μ (Mo- K_α) = 4.53 cm $^{-1}$, $F(000) = 1998$, 26629 reflections in $h(-16/16)$, $k(-16/18)$, $l(-29/30)$, measured in the range $2.05^\circ \leq \theta \leq 27.49^\circ$, completeness $\theta_{\text{max}} = 99.4\%$, 9417 independent reflections, $R_{\text{int}} = 0.0975$, 5582 reflections with $F_o > 4\sigma(F_o)$, 599 parameters, 1 restraints, $R_{1\text{obs}} = 0.0639$, $wR_{2\text{obs}} = 0.1265$, $R_{1\text{all}} = 0.1332$, $wR_{2\text{all}} = 0.1539$, GooF = 1.007, largest difference peak and hole: $0.747/-0.621$ e Å $^{-3}$.

CCDC-654680 (1) contains the supplementary crystallographic data for this paper. These data can be obtained free of charge from The Cambridge Crystallographic Data Centre via www.ccdc.cam.ac.uk/data_request/cif.

{[Bis(2,2':6',2''-terpyridyl)ruthenium]{1,4-bis(2,6-dipyrazol-1-yl)pyrid-4-yl}benzene}tetrakis(hexafluorophosphate) - [(tpy)Ru(L)Ru(tpy)](PF₆)₄ (2): ^1H NMR (400 MHz, $[\text{D}_6]\text{dmsO}$, 25 °C): $\delta = 6.74$ [t, $^3J_{\text{H,H}} = 2.8$ Hz, 4 H, pz H(4)], 7.34 [dt, $^3J_{\text{H,H}} = 6.4$, $^4J_{\text{H,H}} = 0.8$ Hz, 4 H, tpy H(5), H(5'')], 7.44 [d, $^3J_{\text{H,H}} = 2.0$ Hz, 4 H, pz H(3)], 7.76 [d, $^3J_{\text{H,H}} = 4.2$ Hz, 4 H, tpy H(6), H(6'')], 8.07 [dt, $^3J_{\text{H,H}} = 7.2$, $^4J_{\text{H,H}} = 1.2$ Hz, 4 H, tpy H(4), H(4'')], 8.51 [t, $^3J_{\text{H,H}} = 8.0$ Hz, 2 H, tpy H(4'')], 8.78 [s, 4 H, L-ph], 8.84 [d, $^3J_{\text{H,H}} = 8.0$ Hz, 4 H, tpy H(3), H(3'')], 9.04 [d, $^3J_{\text{H,H}} = 8.0$ Hz, 4 H, tpy H(3'), H(5')], 9.34 [s, 4 H, L-py H(3), H(5)], 9.65 [d, $^3J_{\text{H,H}} = 3.2$ Hz, 4 H, pz H(5)] ppm. ^{13}C NMR (100 MHz, $[\text{D}_6]\text{dmsO}$, 25 °C): $\delta = 107.26$ [L-py C(3), C(5)], 111.53 [pz C(4)], 124.34 [tpy C(3'), C(5')], 125.09 [tpy C(3), C(3'')], 128.40 [tpy C(5), C(5'')], 129.51 [L-ph CH], 134.41 [pz C(5)], 137.19 [tpy C(4')], 138.76 [L-ph C(1)], 139.17 [tpy C(4), C(4'')], 146.89 [pz C(3)], 149.74 [L-py C(2), C(6)], 150.57 [L-py C(4)], 153.77 [tpy C(6), C(6'')], 157.10 [tpy C(2'), C(6')], 159.32 [tpy C(2), C(2'')] ppm. UV/Vis (NO_3^- salt MeOH): $\lambda_{\text{max}} = 273$ ($\pi \rightarrow \pi^*$ tpy), 309 ($\pi \rightarrow \pi^*$ L), 369 (w, $^1\text{MLCT}$ towards L), 453 (s, $^1\text{MLCT}$ towards tpy) nm. MALDI-TOF MS (grid-voltage 80%,

guide wire 0.02%, positive reflector mode): $m/z = 1161.74$ ($[\text{C}_{58}\text{H}_{37}\text{N}_{16}\text{Ru}_2]^+$, $[\text{M} - 5\text{H} - 4\text{NO}_3]$). Micro-ESI (acetonitrile/methanol): $m/z = 1600.8$ ($[\text{C}_{58}\text{H}_{42}\text{F}_{18}\text{N}_{16}\text{P}_3\text{Ru}_2]$, $[\text{M} - \text{PF}_6]$). ESI-TOF (acetonitrile/water, 1:1): m/z (%) = 291.54 (100) $[\text{2} \cdot (\text{PF}_6)_2]^{4+}$, 388.39 (6) $[\text{2}^{3+}]$, 437.04 (35) $[\text{2} \cdot \text{PF}_6]^{3+}$, 728.05, (1) $[\text{2}]^{2+}$. $\text{C}_{58}\text{H}_{42}\text{F}_{24}\text{N}_{16}\text{P}_4\text{Ru} \cdot 4(\text{CH}_3)_2\text{SO}$ (2057.6): calcd. C 38.52, H 3.23, N 10.89, Ru 9.82; found C 38.60, H 3.50, N 10.7, Ru 9.68. Because of the insufficient amount of pure complex $\text{2} \cdot (\text{PF}_6)_4$, the sample used for elemental analysis was precipitated with hexane from a NMR-pure $[\text{D}_6]\text{dmsO}$ solution in order to remove excessive dmsO by extraction with water. Residual solvent was removed at elevated temperature in vacuo.

Supporting Information (see footnote on the first page of this article): Original mass spectrometric analysis spectra, 1D and 2D NMR spectra, square-wave voltammograms and low-temperature emission spectra.

Acknowledgments

The authors thank the Deutsche Forschungsgemeinschaft (DFG) for financial support within the frame of the project "Inducing charge states in single molecule junctions" DFG-SPP 1243. Velimir Meded is acknowledged for his help in the preparation of the manuscript. Furthermore, the authors thank Oliver Hampe and Verena Tellström for the measurement of the ESI-TOF spectra and Sergei Lebedkin for the low-temperature emission spectroscopy measurements. We are grateful to the referees who gave helpful advices for this manuscript.

- a) V. Balzani, A. Juris, M. Venturi, S. Campagna, S. Serroni, *Chem. Rev.* **1996**, *96*, 759–833; b) S. Campagna, F. Puntiero, N. Nastasi, G. Baergamini, V. Balzani, *Top. Curr. Chem.* **2007**, *280*, 117–214.
- J. P. Sauvage, J. P. Collin, J. C. Chambron, S. Guillerez, C. Coudret, V. Balzani, F. Barigelletti, L. De Cola, L. Flamigni, *Chem. Rev.* **1994**, *94*, 993–1019.
- a) H. Inoue, S. Funyu, Y. Shimada, S. Takagi, *Pure Appl. Chem.* **2005**, *77*, 1019–1033; b) K. L. Wouters, N. R. de Tacconi, R. Konduri, R. O. Lezna, F. M. MacDonnell, *Photosynth. Res.* **2006**, *87*, 41–55.
- S. Rau, B. Schäfer, D. Gleich, E. Anders, M. Rudolph, M. Friedrich, H. Görls, W. Henry, J. G. Vos, *Angew. Chem. Int. Ed.* **2006**, *45*, 6215–6218.
- a) J. A. Faiz, R. M. Williams, M. J. J. Pereira Silva, L. De Cola, Z. Pikramenou, *J. Am. Chem. Soc.* **2006**, *128*, 4520–4521; b) J. M. Haider, R. M. Williams, L. De Cola, Z. Pikramenou, *Angew. Chem. Int. Ed.* **2003**, *42*, 1830–1833; c) H. Wolpher, S. Sinha, J. X. Pan, A. Johansson, M. J. Lundqvist, P. Persson, R. Lomoth, J. Bergquist, L. C. Sun, V. Sundström, B. Åkermark, T. Polivka, *Inorg. Chem.* **2007**, *46*, 638–651; d) M. Borgström, S. Ott, R. Lomoth, J. Bergquist, L. Hammarström, O. Johansson, *Inorg. Chem.* **2006**, *45*, 4820–4829.
- R. T. F. Jukes, B. Zozic, F. Hartl, P. Belsler, L. De Cola, *Inorg. Chem.* **2006**, *45*, 8326–8341.
- a) Md. K. Nazeeruddin, S. M. Zakeeruddin, J. J. Lagref, P. Liska, P. Comte, C. Barolo, G. Viscardi, K. Schenk, M. Graetzel, *Coord. Chem. Rev.* **2004**, *248*, 1317–1328; b) Md. K. Nazeeruddin, C. Klein, P. Liska, M. Graetzel, *Coord. Chem. Rev.* **2005**, *249*, 1460–1467; c) F. T. Kong, S. Y. Dai, K. J. Wang, *Chin. J. Chem.* **2007**, *25*, 168–171.
- a) J. D. Badjic, C. M. Ronconi, J. F. Stoddart, V. Balzani, S. Silvi, A. Credi, *J. Am. Chem. Soc.* **2006**, *128*, 1489–1499; b) A. Petitjean, F. Puntiero, S. Campagna, A. Juris, J. M. Lehn, *Eur. J. Inorg. Chem.* **2006**, *19*, 3878–3892; c) V. Balzani, G. Bergamini, F. Marchioni, P. Ceroni, *Coord. Chem. Rev.* **2006**,

- 250, 1254–1266; d) S. Nitahara, N. Terasaki, T. Akiyama, S. Yamada, *Thin Solid Films* **2006**, *499*, 354–358.
- [9] a) M. Ruben, S. Rau, A. Skirl, K. Krause, H. Görls, D. Walther, J. G. Vos, *Inorg. Chim. Acta* **2000**, 206–214; b) F. Schramm, H. Görls, D. Walther, *Z. Anorg. Allg. Chem.* **2006**, *632*, 391–399; c) F. Schramm, D. Walther, H. Görls, C. Käßlinger, R. Beckert, *Z. Naturforsch.* **2005**, *60b*, 843–852; d) M. Schmittel, H. W. Lin, E. Thiel, A. J. Meixner, H. Ammon, *Dalton Trans.* **2006**, 4020–4028.
- [10] a) S. Bonnet, J. P. Collin, M. Koizumi, P. Mobian, J. P. Sauvage, *Adv. Mater.* **2006**, *18*, 1239–1250; b) V. Balzani, A. Credi, S. Silvi, M. Venturi, *Chem. Soc. Rev.* **2006**, *35*, 1135–1149.
- [11] a) W. R. Browne, N. M. O’Boyle, W. Henry, A. L. Guckian, S. Horn, T. Fett, C. M. O’Connor, M. Duati, L. De Cola, C. G. Coates, K. L. Ronayne, J. J. McGarvey, J. G. Vos, *J. Am. Chem. Soc.* **2005**, *127*, 1229–1241; b) W. R. Browne, R. Hage, J. G. Vos, *Coord. Chem. Rev.* **2006**, *250*, 1653–1668.
- [12] B. Dietzek, W. Kiefer, J. Blumhoff, L. Böttcher, S. Rau, D. Walther, U. Uhlemann, M. Schmitt, J. Popp, *Chem. Eur. J.* **2006**, *12*, 5105–5115.
- [13] a) M. I. J. Polson, F. Loiseau, S. Campagna, G. S. Hanan, *Chem. Commun.* **2006**, 1301–1303; b) E. A. Medlycott, G. S. Hanan, *Coord. Chem. Rev.* **2006**, *250*, 1763–1782; c) E. A. Medlycott, G. S. Hanan, *Chem. Soc. Rev.* **2005**, *34*, 133–142.
- [14] D. L. Jameson, J. K. Blaho, K. T. Kruger, K. A. Goldsby, *Inorg. Chem.* **1989**, *28*, 4312–4314.
- [15] Surprisingly, the heteroleptic complex Ru(bpp)tpy exhibits only one ¹MLCT band at 430 nm “indicating strong coupling between the π^* orbitals of the mixed ligand complex” according to ref.^[14]
- [16] F. Kröhnke, *Synthesis* **1976**, 1–24.
- [17] D. G. Kurth, F. Caruso, C. Schüler, *Chem. Commun.* **1999**, 1579–1580.
- [18] E. C. Constable, A. M. W. Cargill Thompson, *J. Chem. Soc., Dalton Trans.* **1992**, 3467–3475.
- [19] a) J. P. Collin, P. Lainé, J. P. Launay, J. P. Sauvage, A. Sour, *J. Chem. Soc., Chem. Commun.* **1993**, 434–435; b) L. Hammarström, F. Barigelletti, L. Flamigni, M. T. Indelli, N. Armadori, G. Calogero, M. Guardigli, A. Sour, J. P. Collin, J. P. Sauvage, *J. Phys. Chem. A* **1997**, *101*, 9061–9069; c) M. T. Indelli, F. Scandola, J.-P. Collin, J. P. Sauvage, A. Sour, *Inorg. Chem.* **1996**, *35*, 303–312; d) ttpy is 4'-p-tolyl-2,2':6,2''-terpyridine, and tpy-ph-tpy is 1,4-bis(2,2':6,2''-terpyridin-4'-yl)benzene.
- [20] F. Barigelletti, L. Flamigni, M. Guardigli, J. P. Sauvage, J. P. Collin, A. Sour, *Chem. Commun.* **1996**, 1329–1330.
- [21] a) F. Barigelletti, L. Flamigni, V. Balzani, J. P. Collin, J. P. Sauvage, A. Sour, E. C. Constable, A. M. W. Cargill Thompson, *J. Am. Chem. Soc.* **1994**, *116*, 7692–7699; b) M. Abrahamsson, H. Wolpher, O. Johansson, J. Larsson, M. Kritikos, L. Eriksson, P. O. Norrby, J. Bergquist, L. Sun, B. Åkermark, L. Hammarström, *Inorg. Chem.* **2005**, *44*, 3215–3225.
- [22] V. V. Pavlishchuk, A. W. Addison, *Inorg. Chim. Acta* **2000**, *298*, 97–102. The authors used a +0.38 V addition for the adaptation of SCE vs. ferrocene and a +0.384 V addition towards SSCE values.
- [23] T. E. Janini, J. L. Fattore, D. L. Mohler, *J. Organomet. Chem.* **1999**, *578*, 260–263.
- [24] S. Văduvescu, P. G. Potvin, *Eur. J. Inorg. Chem.* **2004**, 1763–1769.
- [25] M. Schmittel, V. Kalsani, P. Mal, J. W. Bats, *Inorg. Chem.* **2006**, *45*, 6370–6377.
- [26] M. Schmittel, V. Kalsani, R. S. K. Kishore, H. Cölfen, J. W. Bats, *J. Am. Chem. Soc.* **2005**, *127*, 11544–11545.
- [27] Y. Bodenthin, U. Pietsch, H. Möhwald, D. G. Kurth, *J. Am. Chem. Soc.* **2005**, *127*, 3110–3115.
- [28] H. Torieda, A. Yoshimura, K. Nozaki, S. Sakai, T. Ohno, *J. Phys. Chem. A* **2002**, *106*, 11034–11044.
- [29] A. J. Downard, G. E. Honey, P. J. Steel, *Inorg. Chem.* **1991**, *30*, 3733–3737.
- [30] a) M.-A. Haga, N. Kato, H. Monjushiro, K. Wang, Md. D. Hossain, *Supramol. Sci.* **1998**, *5*, 337–342; b) M.-a. Haga, T. Takasugi, A. Tomie, M. Ishizuya, T. Yamada, Md. D. Hossain, M. Inoue, *Dalton Trans.* **2003**, 2069–2079; c) M.-a. Haga, M. Ohta, H. Machida, M. Chikira, N. Tonegawa, *Thin Solid Films* **2006**, *499*, 201–206; d) B. Mondal, S. Chakraborty, P. Munshi, M. G. Walawalkar, G. K. Lahiri, *J. Chem. Soc., Dalton Trans.* **2000**, 2327–2335.
- [31] a) M. Duati, S. Tasca, F. C. Lynch, H. Bohlen, J. G. Vos, S. Stagni, M. D. Ward, *Inorg. Chem.* **2003**, *42*, 8377–8384; b) M. Duati, S. Fanni, J. G. Vos, *Inorg. Chem. Commun.* **2000**, *3*, 68–70.
- [32] a) O. Johansson, R. Lomoth, *Chem. Commun.* **2005**, 1578–1580; b) H. Wolpher, O. Johansson, M. Abrahamsson, M. Kritikos, L. C. Sun, B. Åkermark, *Inorg. Chem. Commun.* **2004**, *7*, 337–340.
- [33] a) R. P. Thummel, V. Hegde, Y. Jahn, *Inorg. Chem.* **1989**, *28*, 3264–3267; b) Y. Jahng, S. W. Moon, R. P. Thummel, *Bull. Korean Chem. Soc.* **1997**, *18*, 174–185; c) A. Winter, J. Hummel, N. Risch, *J. Org. Chem.* **2006**, *71*, 4862–4871.
- [34] a) V. A. Money, I. Radosavljevic Evans, M. A. Halcrow, A. E. Goeta, J. A. K. Howard, *Chem. Commun.* **2003**, 158–159; b) J. M. Holland, J. A. McAllister, C. A. Kilner, M. Thornton-Pett, A. J. Bridgeman, M. A. Halcrow, *J. Chem. Soc., Dalton Trans.* **2002**, 548–554; c) C. Carbonera, J. Sánchez Costa, V. A. Money, J. Elhaik, J. A. K. Howard, M. A. Halcrow, J. F. Létard, *Dalton Trans.* **2006**, 3058–3066; d) N. K. Solanki, E. J. L. McInnes, F. E. Mabbs, S. Radojevic, M. McPartlin, N. Feeder, J. E. Davies, M. A. Halcrow, *Angew. Chem. Int. Ed.* **1998**, *37*, 2221–2223; e) T. Ayers, S. Scott, J. Goins, N. Caylor, D. Hathcock, S. J. Slattery, D. L. Jameson, *Inorg. Chim. Acta* **2000**, *307*, 7–12.
- [35] a) J. M. Holland, J. A. McAllister, Z. Lu, C. A. Kilner, M. Thornton-Pett, M. A. Halcrow, *Chem. Commun.* **2001**, 557–560; b) C. Rajadurai, F. Schramm, S. Brink, O. Fuhr, M. Ghafari, R. Kruk, M. Ruben, *Inorg. Chem.* **2006**, *45*, 10019–10021; c) C. Rajadurai, O. Fuhr, R. Kruk, M. Ghafari, H. Hahn, M. Ruben, *Chem. Commun.* **2007**, 2636–2638.
- [36] B. P. Sullivan, J. M. Calvert, T. J. Meyer, *Inorg. Chem.* **1980**, *19*, 1404–1407.
- [37] H. Friebolin, *Basic One- and Two-Dimensional NMR Spectroscopy*, Wiley-VCH Weinheim (Germany), **2005**, 4th rev. ed..
- [38] H. Elsbernd, J. K. Beattie, *J. Inorg. Nucl. Chem.* **1972**, *34*, 771–774.
- [39] J. Elguero, A. Fruchier, A. De La Hoz, F. A. Jalón, B. R. Manzano, A. Otero, F. Gómez-De La Torre, *Chem. Ber.* **1996**, *129*, 589–594.
- [40] A. C. Laemmel, J. P. Collin, J. P. Sauvage, *C. R. Acad. Sci. Paris, Série IIc, Chemistry* **2000**, 43–49; therein: ttpy = 4'-tolyl-2,2':6':2''-terpyridine, dmpp = 2,6-bis(3,5-dimethyl-N-pyrazolyl)pyridine.
- [41] J. P. Lecomte, A. Kirsch-De Mesmaeker, G. Orellana, *J. Phys. Chem.* **1994**, *98*, 5382–5388.
- [42] D. Walther, L. Böttcher, J. Blumhoff, S. Schebesta, H. Görls, K. Schmuck, S. Rau, M. Rudolph, *Eur. J. Inorg. Chem.* **2006**, *12*, 2385–2392.
- [43] R. Hage, R. Prins, J. G. Haasnot, J. Reedijk, J. G. Vos, *J. Chem. Soc., Dalton Trans.* **1987**, 1389–1395.
- [44] a) B. P. Sullivan, D. J. Salmon, T. J. Meyer, J. Peedin, *Inorg. Chem.* **1979**, *18*, 3369–3374; b) M. L. Stone, G. A. Crosby, *Chem. Phys. Lett.* **1981**, *79*, 169–173.
- [45] P. J. Steel, F. Lahousse, D. Lerner, C. Marzin, *Inorg. Chem.* **1983**, *22*, 1488–1493.
- [46] a) M. Ruben, *Angew. Chem. Int. Ed.* **2005**, *44*, 1594–1596; b) N. Lin, S. Stepanow, F. Vidal, K. Kern, M. S. Alam, S. Strömsdörfer, V. Dremov, P. Müller, A. Landa, M. Ruben, *Dalton Trans.* **2006**, 2794–2800.
- [47] G. P. Moss, P. A. S. Smith, D. Tavernier, *Pure Appl. Chem.* **1995**, *67*, 1307–1375.
- [48] G. Gritzner, J. Kuta, *Pure Appl. Chem.* **1982**, *54*, 1527–1532.

- [49] M. Rudolph, *J. Comput. Chem.* **2005**, *26*, 1193–1204 and references cited therein.
- [50] *COLLECT*, Data Collection Software, Nonius B. V., Netherlands, **1998**.
- [51] Z. Otwinowski, W. Minor, *Methods Enzymol.* **1997**, *276*, 307–326.
- [52] G. M. Sheldrick, *Acta Crystallogr., Sect. A* **1990**, *46*, 467–473.
- [53] G. M. Sheldrick, *SHELXL-97* (Release 97–2), *Program for the Refinement of Crystal Structures*, University of Göttingen, Germany, **1997**.

Received: June 20, 2008
Published Online: November 28, 2008